

Experimental Demonstration of High-Sensitivity Nano capacitors via Advanced Nanofabrication Techniques for Nano Electronic Implementations

Haider Alrudainy^{a*}, Muaad Hussein^a, U. Hashim^b, Adam Tijjani^c, and TS. Naser^b

^a Basra Engineering Technical College, Southern Technical University, Basra, Iraq

^b Institute of Nano Electronic Engineering, University Malaysia Perlis, Perlis, 01000 Kangar, Malaysia

^c Faculty of Technology, University Malaysia Perlis (UniMAP), Kampus Uniciti Alam Sg. Chuchuh, 02100 Padang Besar (U), Perlis, Malaysia

* Corresponding author. Tel.: +964-771-089-2417; fax: +0-000-000-0000; e-mail: h.m.a.alrudainy@stu.edu.iq

Received 28 January 2023, Revised 8 May 2023, Accepted 17 July 2023

ABSTRACT

Nano gap capacitors have recently received significant interest as a key component in a wide range of implementations including photonics, Nanoelectronics, and sensing applications. Many exploratory research projects are being conducted to investigate the electrical characteristics of these nano capacitors. One essential issue that this paper addresses is the need for highly sensitive nano gap capacitors which can be adopted for ultra-low power sensing implementations. In this paper, gold is utilized as the electrode material owing to its superb chemical stability, electrical conductivity, and biocompatibility. The fabrication process is started by designing the mask namely nano gap pad electrodes using AutoCAD software. Subsequently, the designs are finally transferred and fabricated onto a chrome glass surface. In this work, after a combination of conventional photolithography and size reduction approach used to fabricate the device, conventional photolithography is applied to transfer the nano gap pattern onto the gold surface. In order to achieve the desired dimension of the nano gap, a size reduction technique is employed. Describe the most important thing in 2-3 sentences only). Visual inspection using a High Power Microscope (HPM), 3D nano profiler, X-Ray diffractions (XRD), and Field Emission Scanning Electron Microscope (FESEM) have been employed to observe and validate the fabricated structures. Results show that a 2.5 nano Ampere is measured as the applied voltage increases to 10 mV. This firmly demonstrates the ultra-low power consumption, several Pico watts, of these nano gap capacitors. Further, our findings show that the fabricated 4nm gap structure can achieve an approximately 300 nano farad capacitor at low frequencies, which is advantageous for adoption in highly sensitive biosensors.

Keywords: gold electrodes, nano gaps capacitor, size reduction technique, and Nanoelectronic

1. INTRODUCTION

Over recent years, there has been substantial research in the fabrication and testing of high-frequency micro-electro-mechanical system (MEMS) resonators, whereby significant progress has recently been achieved [1]. In the case of parallel plate electrostatic transducers, increasing the resonant frequency of MEMS resonators to the gigahertz scale often causes the gap spacing between the resonator and the electrodes to diminish. Dimension of the gap of less than 100nm for films thickness larger than 2 μ m (of aspect ratio \sim 25 to 1) is required to minimize the kinetic resistance, accordingly decreasing the insertion loss of the device. Such an aggressive requirement has recently been employed with the photoresist etching technique [2]. However, the gap dimension achieved, for the most part, was still greater than 100nm. Many other fabrication techniques have been previously proposed and demonstrated to optimize the gap size between the electrodes [3-5]. Nano gap is extensively investigated because these transducers can operate in an on-off manner, which allows them to have improved sensing proficiencies, comprising rapid response, short recovery time, high sensitivity, and efficient reliability [6]. In addition, this investigation, for instance, includes conduction of electricity or storage of charge which leads

to an improvement in capacitive behavior [7]. For most of the measurements to be performed an electric voltage can be applied over the two electrodes causing the existence of an increment of free electrons in the material of nano gap dimension, as it is reported in [8].

Nowadays, the nanostructure is considered as an important part in the detection of chemicals and biomolecules because the size of these molecules is less than 10nm. Therefore, any improvements in the fabrication process of these nano gap structures can drastically lead to the incorporation of them in a wide range of nanostructure implementations, especially in biosensor detection. remarkably, the materials are an attractive research area in nanotechnology and biosensor detection, for instance, gold particles can significantly increase the biosensor sensitivity [1].

Improving the methodology of the reproducible and reliable fabrication for nanoscale gaps is totally advantageous because contact electrodes are one of the significant obstacles confronted by molecular electronics. Even though a variety of unconventional techniques has recently progressed over the last few years [9-12], to the

best of our knowledge, there is no practical technique to fabricate nanoscale gaps with spaces in less than 5 nm dimensions by using the controlled side by side process as demand for manufacturing molecular circuits in very large-scale integration (VLSI). Thus far, the formation of multiple nanoscale gaps demands that each experience the materials regime process separately, a constraint imposing fabrication process is extremely time-consuming for manufacturing of very large complex circuitry. To tackle this challenge, an approach adopting size reduction that allows the simultaneous manufacturing of enormous numbers of nanoscale gaps in a single processing step has been developed [13-15]. Our multi-device approach, as expected, balances the power consumption through the materials regime procedure so that every nanoscale gap encounters size reduction in unison. The ultimate design characteristic is that the inter-junction impedance is maintained below the junction resistance which guarantees that none of the individual nanoscale gaps undergo thermal runaway [16]. It is found that the size reduction technique of the parallel combination of Nano electrodes manufactured in this novel geometry functions similarly to that of single nanoscale gap junctions. This includes approximately similar processing time, voltage levels, and current that scale with the number of nanoscale gaps. As an illustration, this process has been adopted to fabricate nanoscale gaps with less than 5nm nanoscale gaps in parallel with the same structure.

Otherwise, gold electrodes in combination with an oxide insulator layer/SOI substrate are equally excellent for reducing the complexity of the processing as well as cost. In principle using electron beam lithography for defining the nano gap is simplest but very expensive and processing is more involved [1]. Whereas, controlled etching of the electrode to define inter-electrode separation is much simpler and low cost as compared to e-beam lithography. However, the resultant geometry of the nano gap after controlled wet etching of the electrode material is much smoother as compared to that involving only one step etching in electron beam lithography addition to its offset by the cost and process complexity [1-3]. The simple planar nano gap fabrication using SOI wafer, conventional optical lithography, and wet etching of Au material and the use of Ti layer as sacrificial or combination of Titanium and gold metallization is a viable and economical way of producing these Nano biosensors at affordable cost. In the case of the sacrificial layer, it is necessary that the film involved is etched easily, preferably at room temperature and the etching rate should be higher so that the sacrificial layer is dissolved before the etchant starts affecting other structural layers used [1-3]. Even if one is able to dissolve this layer, one has to heat the etchant which is bound to affect other thin films already present in the fabricated structure.

2. MATERIAL AND METHODS

2.1. Mask Design

A 100-mm p-type SOI wafer is utilized as a substrate to manufacture the nanoscale gap structure (Si Thickness 1200nm, SiO₂ = 150 ± 5nm, Si = 15 μm) as shown in Figure 1. After we design a mask for the gold

nano gap terminals by using the AutoCAD simulation toolbox, the mask is printed onto a chrome glass surface. It is worth noting that this mask is obtained from a commercial corporation named (Photonic Pte. Limited, Singapore) [17]. Wet etching is applied to fabricate the desired gap and pattern the electrode structures by using an aqua regia solution (HCl 1:3 HN₃). The designed mask for nano gap generation comprises 160 dies with 6 various layouts. The angle dimension at the end electrode is of 1/6th scale beginning from 100 μm, with an increment step of 100 μm, to 1100 μm for every unit of length [18]. This process has been adopted to simply investigate the optimum angle dimension for the perfect nano gap formation after the etching process. In our work, the angle dimension which has been adopted is presented as shown in Figure 2(f).

2.2. Fabrication of Nano Gap Structure

The fabrication process flow of gold nanoscale gap electrodes with the preferred scale of gap regime on the insulator-silicon substrate is schematically demonstrated in Figure 1. Cleaning the SOI wafer is the first step in the fabrication process, before depositing 100nm SiO₂ as an insulator layer for the coming design, using PECVD equipment, as illustrated in Figure 2(a). This step is followed by the evaporation of the 120nm Ti layer as a sacrificial layer, and also to enhance the adhesion between the silicon oxide substrate and the coming gold layer as demonstrated in Figure 2(b), before evaporating 200nm Au layer as can be seen in Figure 2(c). The next is the photolithography process, where a 1200nm thickness layer of positive photoresist is employed on the Au/Ti layers as illustrated in Figure 2(d), and then it is exposed to ultraviolet light across the designed chrome mask. After the development process, the uncovered area will remain intact as shown in Figure 2(e). Subsequently, a wet etching for the Ti/Au substrate is applied using aqua regia solution, by controlling the etched time to get the desired size of gap as demonstrated in Figure 2(f). Finally, the regime nano gap electrodes are applied and fabricated using gold material on the SOI substrate as shown in Figure 2(f). The proposed structures are optically characterized with a ZEISS FESEM ULTRA55 for the pre and post-wet etching process.

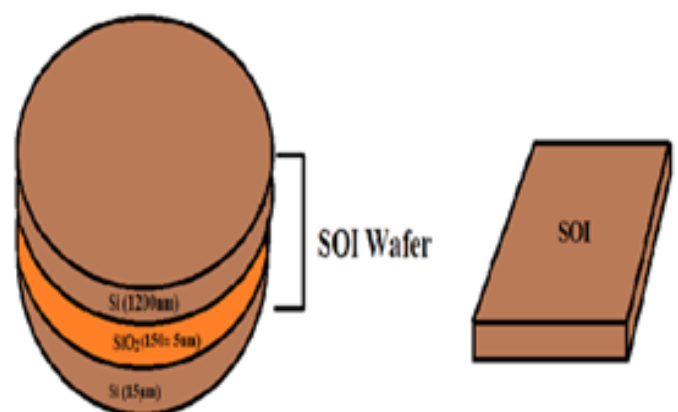


Figure 1. Cross sectional view of SOI wafer with thicknesses labelled

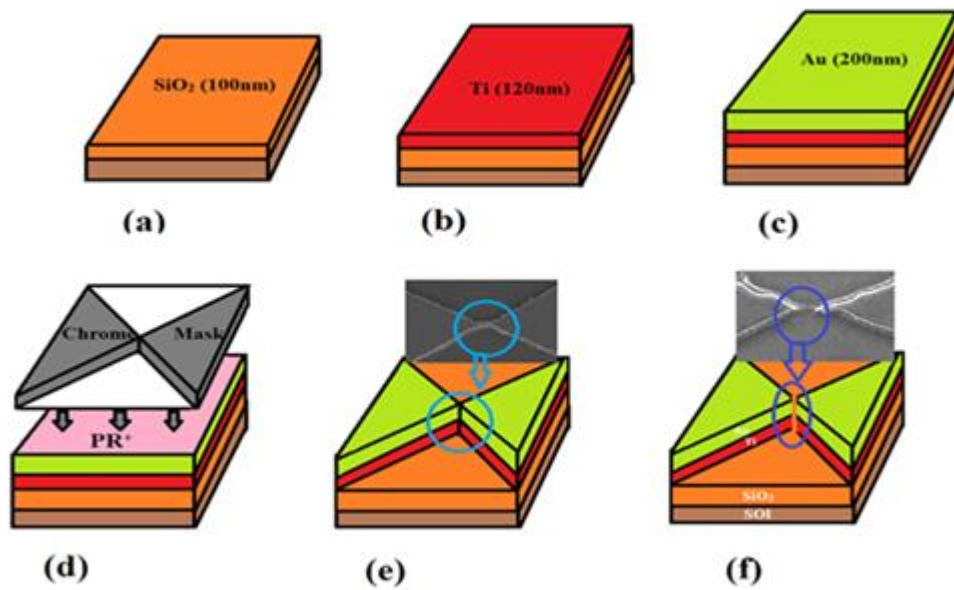


Figure 2. Cross-sectional view of the proposed fabrication process flow of Au/Ti nano gap structure: (a) deposition of 100nm SiO₂ layer, (b) Ti deposition layers, (c) Au 200nm deposition layer, (d) chrome mask exposure and photoresist removing from Au/Ti structure, (e) uncovered area remain intact with zero gap dimension, and (f) gold nano gaps after aqua regia wet etching.

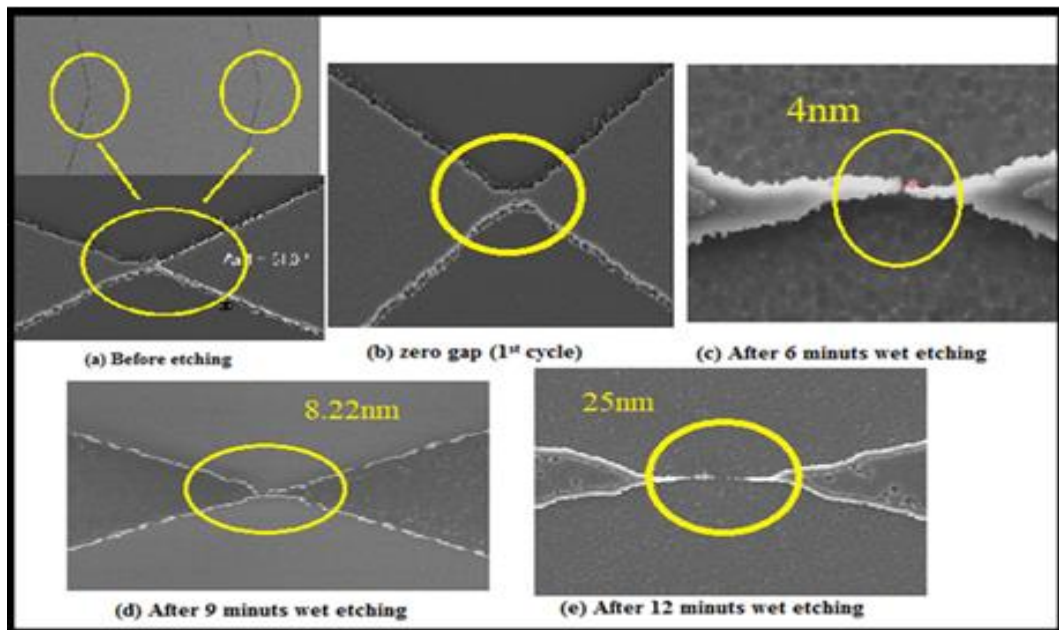


Figure 3. Designation of desired gap; (a) before wet etching, (b) 1st cycle of 3 minutes wet etching using Aqua Regia, (c) the desired 4nm gap after 2nd cycle of 6 minutes wet etching, and Finally, (d) and (e) before consuming the etching time with 9mins, 12mins to get 8nm and 25nm gaps respectively.

2.3. Electrical Characterization

The proposed devices with less than 30nm of gap length have been applied to a Dielectric Analyzer (Alpha-A High Performance Frequency Analyzer, Novocontrol Technologies, Handsangen, Germany), as shown in Figure

3. It is worth mentioning that electrical characteristics including capacitance, resistivity, conductivity, and permittivity are quantified at room temperature with air in the nanoscale gap spaces. In addition, for future work, it can be characterized with different materials and solution percentages to show the whole performance and

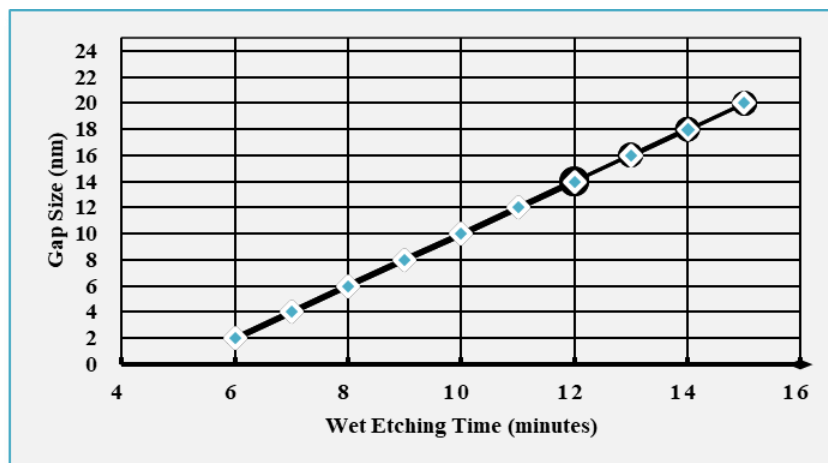


Figure 4. Demonstrates that the gap size rises with the time of the wet etching process

determine the required criteria for biosensor application and biomolecule detection.

3. RESULTS AND DISCUSSIONS

This paper discusses developing an approach via optimizing the fabrication process for reliable nanoscale gaps on very large-scale arrays at a desired length of less than 5nm with superior reproducibility and yield. In addition, this research discusses integrating nanoscale components within them. Primarily, in the cleanroom, metallic gaps on silicon (Si) substrates have been demonstrated, as their properties were widely known. For instance, metals such as gold do not visibly corrode, nor incorporate depletion region. In this study, a recently devised approach has been optimized for carving materials made from a layer with well-controlled thickness. This facilitates the fabrication of arrays of nanoscale gaps in the range of 4–25nm. Gold gap arrays have been optimized to achieve relatively adequately sized gaps without excessive leakage current. Wet etching with a number of 2-3 cycles was applied on the fabricated structure using aqua regia solution with time controlled as shown in Figure 3.

A selective approach to produce nanoscale gaps of width lower than 5nm, analogous to the dimension of nanocrystals and conjugated organic molecules, has been proposed and a patent has been granted. In this work, we have reliably produced nanoscale gaps between Au/Ti electrodes of nearly 2nm to 20nm depending on the time for the wet etching process as can be seen in Figure 4. However, the schematic shows an increment in the gap dimensions during the etching time. The fabricated nano gap structure with 2nm has been characterized optically using a 3D-Nano profiler and XRD detector to confirm the size of the gap and the sequence of the sandwich layers respectively, as shown in Figure 5, before applying the electrical characterization process.

In Figure 5(a) using an interference microscope, a microscopic surface is measured in three dimensions. For scale, the three-dimensional surface measurement above maps characterize within a 20-nanometer range of height, and the designated pit defect is lower than 8 nanometers deep. Notably, the area of the measured microscopic surface is 100×200 microns. Defects, however, may appear either in material surfaces during processing or

afterward upon usage. Therefore, failure analysis is crucial for yielding detailed information to enhance the efficiency, effectiveness, and durability of the surfaces. Moreover, optical surface measurement approaches have been adopted, in this work, to observe these and other physical-quality surfaces including reflectivity, and the roughness of the design edges which is demonstrated significantly perfect as we utilized gold material. In the figure of a 3-dimension surface map as can be seen above, a little of pits present in a step height calibration standard, which is made of quartz and then plated with chrome. These pits may occur as a result of physical processes or chemical impacts. If enough of these pits have appeared, the surface's appropriateness as a step-high standard can be compromised. Optical profilers should be capable of resolving the defect adequately to designate its sizes and to characterize its height or depth as illustrated in Figure 5(a). However, XRD has been used to identify the nanocrystal phases present in a material and thereby reveal chemical composition information as seen in Figure 5(b), while, showing the sequence of the layers approximately in the fabricated nano gap device.

Au/Ti nano gap fabrication will be examined, adopting various chemical treatments to activate the nano gap in future work. Currently, current-voltage (I-V) properties have been measured of such nano gaps, with a tiny contact area to reduce leakage current impacts, without incorporated nanocrystals. In this study, the leakage currents have been investigated, and it is shown that they are not presented with gold nano gap electrodes. For the proposed device, an electrical characteristics model (I-V) has been developed and optimized, as can be shown in Figure 6.

The fabricated nanoscale gap structure was electrically characterized using a Dielectric Analyzer to measure its current-voltage response as shown in Figure 6. An interesting current-voltage (I-V) characteristic has been demonstrated in this study for each gap, which significantly reveals the charge and discrete-energy levels in the nanoscale array elements. The properties of I-V for several devices comprising nanocrystals at nanoscale diameters illustrate steps, indicative of quantized energy levels within the nanoscale gap structure, or Coulomb blockade of an electron tunneling through a double barrier structure.

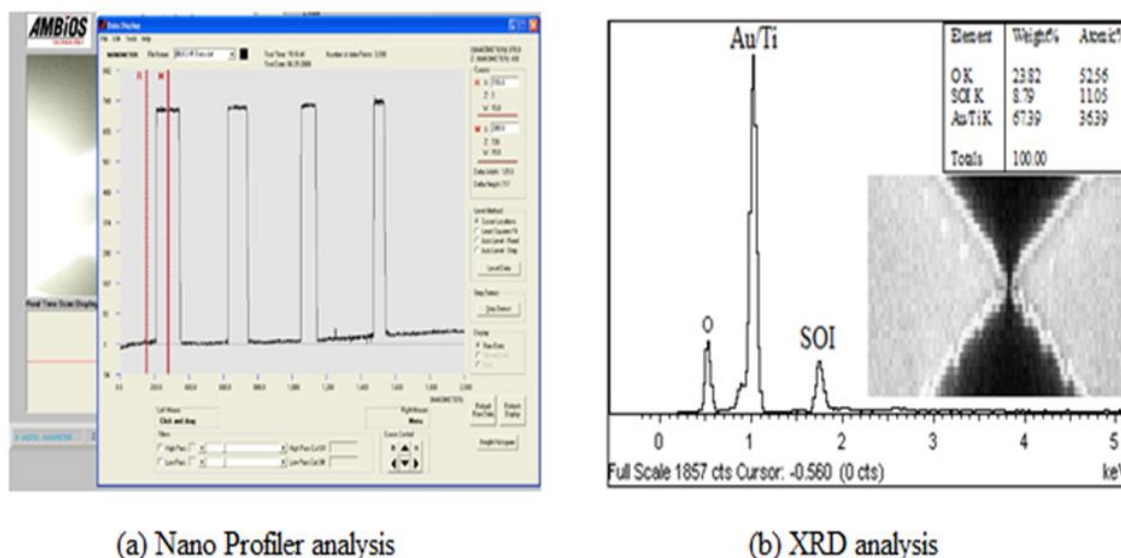


Figure 5. Optical characterization of nano gap structure fabrication using: (a) 3D-Nano profiler, (b) X-Ray Diffraction.

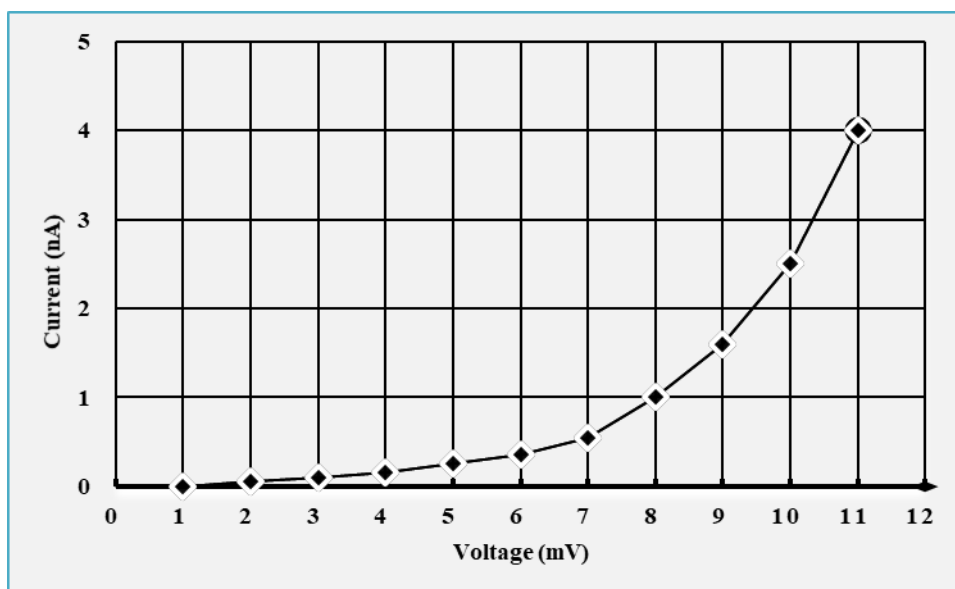


Figure 6. I-V characterization for the nano gap structure fabrication.

This sort of switching behavior can be advantageous in electronic components or it can be adopted in ultra-power consumption implementations, as it can be demonstrated in figure 6. This figure significantly illustrates a drastic increment of current for a specific range of voltages, in which a current of 2.5 Nano amperes has been measured at a voltage equal to 0.01V. However, the functioning devices are the major challenges, and the inadequate reproduction for the specified sample, and between equivalent samples, but the overall behavior for a nanoscale gap fabricated device of sample is consistent. In this work, the characteristics of less than 5nm nanoscale gaps have been studied, to significantly reduce the leakage current through the supporting space insulator. Further, an approach of employing the selectively etched gap served as a template to form a gap between the metal electrodes even optimized the selected materials have been developed [19-20]. This facilitates the prospect of effortless attachment of molecules between the gold electrodes, without necessitating implementing sophisticated chemistry to attach the molecules directly to the nano gap structure.

It has been proven that nano gap electrochemical sensors are superior among several approaches used to detect the presence of biomolecules in different morphologies including chemically compatible variants. Especially, molecular species having dimensions in the range of a few nanometres influence the electrochemical conditions to a nano gap very prominently causing an improved detection without involving labeling as employed in other techniques. The comparative magnitude of influence of these two conditions i.e. ionic properties and double layer formation as mentioned above is decided by the actual inter-electrode separation and the geometrical configuration of the gap. However, the improvement of gold materials and the planar geometry design of the nano gap device may confuse these two requirements. Supplementary, in the case of the planar type of nano gap, using some kind of FESEM imaging is also advantageous to ascertain the presence of molecular species along with the detection of electrochemical variations relying on either admittance or conductance variations. In this context, planar type nano gap is better versatile for detection

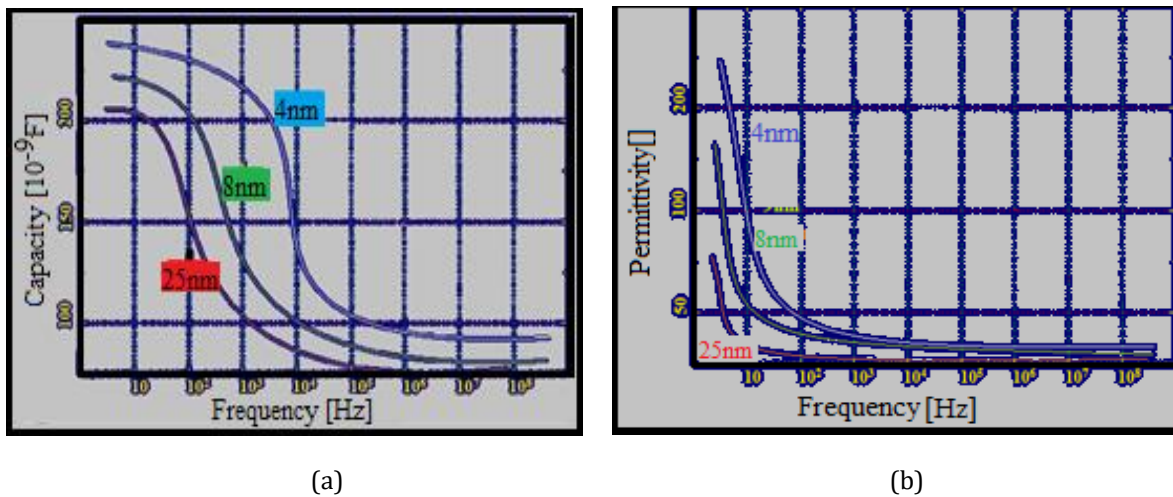


Figure 7. (a) Capacitance-Frequency, and (b) Permittivity-frequency analysis for the fabricated three sizes of nano gap.

point of view compared with the other geometrical designs.

In a biosensor application, the advantages of a nanoscale sensor are ultimately estimated by the following parameters. Ease in fabrication, flexibility in designing different inter-electrode gaps, compatibility of materials of the electrode with the molecular kinds under study, reuse of sensing elements by easily eliminating the electrolyte in the prior measurement [21], higher sensitivity, and finally the cost. Various methods used to fabricate nano gap structures ultimately indicate towards the supremacy of the method based on CMOS processing involving conventional IC processes. The use of gold electrodes shows advantages in several cases including better affinity to DNA strands by thiol radical attachment as will be confirmed in future work.

In this case, the structure is a metal oxide semiconductor and the capacitance has been characterized, as shown in Figure 7 (a), to show the effects of the upper and lower frequencies responding with different sizes of gaps 4, 8, and 25nm of gold nano gap structure. However, the applied voltage at the electrodes will be influenced by the metal of the electrodes because the carriers are one type on which the electric field (E-field) is terminating. Under these conditions, an MOS capacitor is considered as the valance band that is closer or interface to the conduction, and thus electrons are donated or accepted easily to move through the conduction area. Moreover, a parametric study has been performed to show the effect of gap size on capacitance as demonstrated in Figure 7 (a). Capacitance-frequency curves, as shown in Figure 7 (a), at different sizes of gaps provide a great deal of information about the nano gaps structure which is of primary interest when one investigates the MOS process.

In low-frequency area $>10\text{Hz}$ or quasi-static measurement sustains thermal balance at all times. This capacitance can be estimated by dividing the charge rate over the change in applied voltage while the capacitor is in balance at each voltage for this range of low frequency. A typical measurement has been implemented with a dielectric analyzer which evaluates the increased charge per unit of period as the frequency changes gradually towards small values.

The frequency range $>10\text{ Hz}$ shows a delay in the capacitance values obtained from measuring the

capacitance of a small signal at a higher frequency. Under such conditions, one finds that the depletion layer affections decreased after using gold materials [22]. Therefore, the high band frequency capacitance indicates the rate of change in charge in the depletion layer and the, even small, movement of the inversion layer charge. Non-ideal impacts in MOS capacitors comprise fixed, surface states and mobile charge. Nevertheless, as the applied voltage is changed, the fermi energy at the oxide-semiconductor substrate between two electrodes interface varies accordingly and impacts the occupancy of the surface states. The transition in capacitance measurement will be less severe due to the interface states. However, the smallest size of gap the less abrupt can be achieved as seen in Figure 7 (a). The evaluation of the surface state density in full measure has been facilitated by the combination of high and low-frequency capacitance.

A significant obstacle to utilizing resistance spectroscopy in sensing the electrode polarization impact arises from the movement of free ions to the electrode-edge interface, forming an electrical double layer (EDL) by different ions classified in the polar fundamentals area. The dielectric response is screened by the electric double layer, and the response of the low-frequency signal is dominated by the dielectric response and large capacitance. It thus conceals the most relevant information about isolated species, including the hybridization of DNA and changes in molecular conformation. The manufacturing of nanoscale gap capacitors with electrode spaces smaller than the EDL thickness would drastically decrease electrode polarization impacts and facilitate tremendous improvement in sensitivity owing to the perfect matching of the sensing volume with the size of the target entities. In this study, the manufacturing of a horizontal thin film nanoscale gaps capacitive sensor with electrode space of less than 5nm, which demonstrates hardly any electrode polarization impacts when measured with water and ionic buffer solutions, has been reported. This will be informed in future works, thereby facilitating direct quantification of their relative dielectric constant at low frequencies.

Moreover, characterization of the permittivity for the nanogap structures with the frequency is the most important step to identify the sensitivity of the fabricated nano gap structure and supports its coming applications with Biosensor detection. However, the permittivity behavior changes with the frequency followed by the

instruction of the capacitance characterization with low and high frequencies related to the following equation:

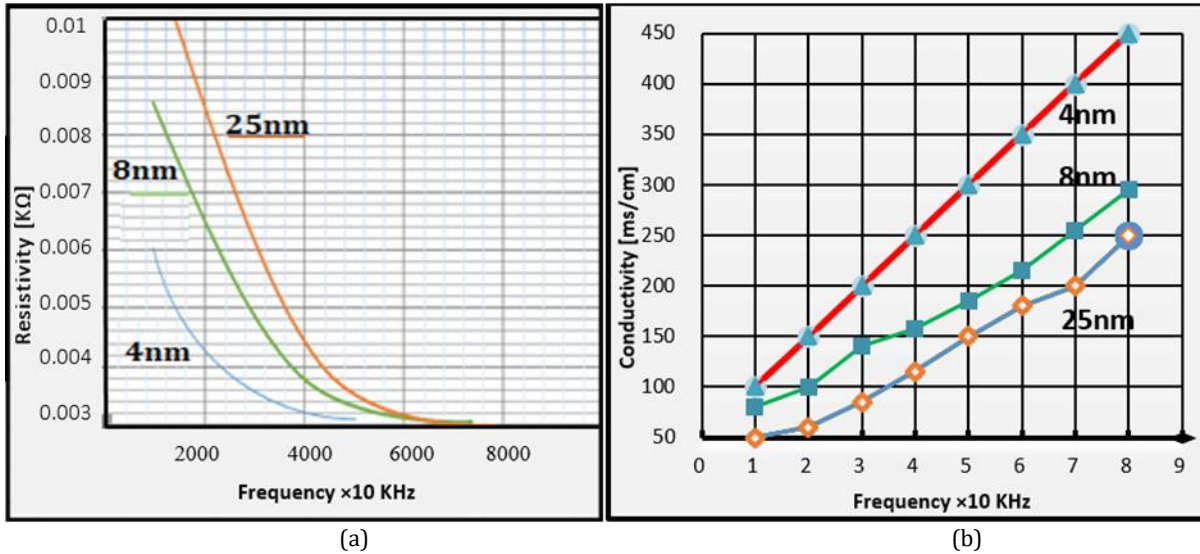


Figure 8. Characterization for different sizes of fabricated nano gap structures: (a) Resistivity, (b) Conductivity.

$$C = \epsilon A/d \quad (1)$$

Where $\epsilon = \epsilon_0 * \epsilon_r$. Here, ϵ_0 illustrates the dielectric constant for air ($\sim 8.854 \times 10^{-12}$ F / m), ϵ_r denotes the relative permittivity of the dielectric materials in the free space between the electrodes, A denotes the surface area of the nanoscale gap electrode structures, C refers the capacitance value, and d represents the length between the two electrodes or the size of the gap. Defiantly, the reduction of gap size should increase the capacitance as well as the permittivity of a nano gap device [23] as shown in Figure 7 (b). The above equation similarly indicates that capacitance (C) and permittivity (ϵ) have a linear relationship, implying that any increase in permittivity leads to an increment in the total capacitance, seeing that permittivity is the numerator of the equation (1).

In Figure 7(b), proceedings at different frequencies illustrate variations in permittivity for the different sizes of the nano gaps structure and measurements of standard deviation across the frequency spectrum. Remarkably, the standard deviation to the bottom in the low-frequency region is high owing to measurement noise at extremely high system impedance. However, at high frequency, system response is constrained by parasitic capacitance, and the dependence on nanoscale gap device is largely decreased the permittivity variations, which is a critical parameter in estimating the opportunity of using nano gap capacitors in an attempt to map changes with the biosensor molecules in detection issues.

In Figure 8, the resistivity represents the capacitive reactance with frequencies variable values as demonstrated in Figure 8(a). However, the permittivity indicates the index of a material's capability to transmit current without incurring an impedance [24]. Conversely, conductivity reflects the substance's capacity to permit the flow of current. Therefore, the conductivity and permittivity are directly proportional. Consequently, any increment in conductivity, and permittivity as can be seen in Figure 8(b) (use the style consistently), with gap-size reduction postulates the fabricated nanoscale gap

structure can be adopted in biosensing implementations with significantly minimum power consumption. While,

the conductivity amount rises progressively as the frequency increases. When the charge alternation increases, the contact between them progressively increases, as a result increasing the conductivity between the two terminals [25].

4. CONCLUSIONS

In this work, an approach has been developed to utilize the selectively etched gap as a template to form a gap between metal plates. Gold is an attractive material to facilitate a well-characterized surface for the self-assembly of elements in nanoscale dimensions terminating in anchor particles. This provides the potential for effortless attachment of molecules to a gold nanostructure, without necessitating the implementation of sophisticated chemistry to embed the molecules directly into the gold electrodes. The accomplishments of this work package are mainly due to advancements in a number of substantially promising approaches for fabricating arrays of nanoscale gaps relatively replicable, and the capability to self-assemble functional molecules and nanocrystals within metal gaps by adopting a size reduction approach. This study, interestingly, has taken a shorter time than predicted, with reproducibility of the measurements being a minimal challenge. Nanocrystals are not stable in such E-field without being anchored in the gap, therefore it is essential to promote mechanisms of embedding them in prestige material such as gold. This capability is similarly necessary to self-assemble molecules in gold nanoscale gaps. Metal evaporation does occur, causing adequately indefectible electrical contacts and significantly minimal surface leakage charges. This can make it a promising candidate for nano gap contact improvement. The fabricated device has been characterized by FESEM, XRD, and electrical measurements. However, the results show decreasing the capacitance with high frequency and this is promising adoption for gold electrode structures of molecular electronic devices comprising either conjugated molecules or nanocrystals. This has demanded the development of substantially smaller nanoscale gaps than

at first predicted, delaying the time in which electrical measurements of the molecules could be made.

ACKNOWLEDGEMENTS

Supporting people and institutions (including Science Foundation) go here. The researchers team and scientific at University Malaysia Perlis and Southern Technical University.

REFERENCES

- [1] L. Wei, X. Kuai, Y. Bao, J. Wei, L. Yang, P. Song, M. Zhang, F. Yang, and X. Wang, "The Recent Progress of MEMS/NEMS Resonators," *Micromachines*, vol. 12, no. 6, p. 724, 2021.
- [2] M.-A. Eyoum, E. Quevy, H. Takeuchi, T. King, and R. T. Howe, "Ashing Technique for Nano-Gap Fabrication of Electrostatic Transducers," *Nontraditional Approaches to Patterning 2*, pp. 145-148, 2004.
- [3] J. R. Clark, W.-T. Hsu, and C. C. Nguyen, "High-Q VHF micromechanical contour-mode disk resonators," in *International Electron Devices Meeting*, 2000, pp. 493-496.
- [4] H. Alrudainy, A. Mokhov, and A. Yakovlev, "A scalable physical model for nano-electro-mechanical relays," in *24th International Workshop on Power and Timing Modeling, Optimization and Simulation (PATMOS)*, 2014, pp. 1-7.
- [5] J. R. Clark, W.-T. Hsu, and C. C. Nguyen, "High-Q VHF micromechanical contour-mode disk resonators," in *International Electron Devices Meeting*, 2000, pp. 493-496.
- [6] T. S. Dhahi, T. Adam, and U. Hashim, "In-House fabrication and Electrical characterization of planner si-nanogap," *Journal of Physics: Conference Series*, vol. 908, no. 1, p. 012064, 2017.
- [7] V. Shukla, N. K. Jena, A. Grigoriev, and R. Ahuja, "Prospects of graphene-hBN heterostructure nanogap for DNA sequencing," *ACS Applied Materials & Interfaces*, vol. 9, no. 46, pp. 39945-39952, 2017.
- [8] M. N. A. Uda, S. C. B. Gopinath, U. Hashim, N. H. Halim, N. A. Parmin, M. N. A. Uda, T. Adam, and P. Anbu, "Silica and graphene mediate arsenic detection in mature rice grain by a newly patterned current-volt aptasensor," *Scientific Reports*, vol. 11, no. 1, p. 14688, 2021.
- [9] M. D. Fischbein and M. Drndić, "Nanogaps by direct lithography for high-resolution imaging and electronic characterization of nanostructures," *Applied Physics Letters*, vol. 88, no. 6, p. 063116, 2006.
- [10] H. Park, A. K. Lim, A. P. Alivisatos, J. Park, and P. L. McEuen, "Fabrication of metallic electrodes with nanometer separation by electromigration," *Applied Physics Letters*, vol. 75, no. 2, pp. 301-303, 1999.
- [11] D. R. Strachan, D. E. Smith, D. E. Johnston, T. H. Park, M. J. Therien, D. A. Bonnell, and A. T. Johnson, "Controlled fabrication of nanogaps by electromigration," *Applied Physics Letters*, vol. 88, no. 6, p. 063116, 2006.
- [12] T. S. Dhahi, T. Adam, S. C. B. Gopinath, and U. Hashim, "Gold nanogap impedimetric biosensor for precise and selective *Ganoderma boninense* detection," *Biotech3*, vol. 12, no. 11, pp. 1-14, 2022.
- [13] T. Adam, T. S. Dhahi, S. C. B. Gopinath, and U. Hashim, "Novel Approaches in Fabrication and Integration of Nanowire for Micro/Nano Systems," *Critical Reviews in Analytical Chemistry*, vol. 1, pp. 1-17, 2021.
- [14] G. K. Ramachandran, M. D. Edelstein, D. L. Blackburn, J. S. Suehle, E. M. Vogel, and C. A. Richter, "Nanometer gaps in gold wires are formed by thermal migration," *Nanotechnology*, vol. 16, no. 8, pp. 1294-1299, 2005.
- [15] T. S. Dhahi and S. Ahmad, "Metal contacts to 2D-materials for device applications," *Electrical and Electronic Technology Open Access Journal*, vol. 2, pp. 31-38, 2018.
- [16] M. Hussein, H. Alrudainy, and W. Abdulkawi, "Bandpass THz Frequency Selective Surface with Flat Passband," *Przeglad Elektrotechniczny*, vol. 98, no. 8, pp. 73-76, 2022.
- [17] A. Salazar et al., "Nanogap fabrication by Joule heating of electromechanically spun suspended carbon nanofibers," *Carbon*, vol. 115, pp. 811-818, 2017.
- [18] A. Salazar et al., "Sub-10 nm nanogap fabrication on suspended glassy carbon nanofibers," *Microsystems & Nanoengineering*, vol. 6, no. 9, 2020.
- [19] J. Hammond, M. Rosamond, S. Sivaraya, F. Marken, and P. Estrela, "Fabrication of a horizontal and a vertical large surface area nanogap electrochemical sensor," *Sensors*, vol. 16, no. 2128, 2016.
- [20] T. Adam, T. S. Dhahi, S. C. B. Gopinath, U. Hashim, and M. N. A. Uda, "Recent advances in techniques for fabrication and characterization of nanogap biosensors: A review," *Biotechnology and Applied Biochemistry*, 2022. DOI: 10.1002/bab.2212.
- [21] A. Aalsaud, H. Alrudainy, R. Shafik, F. Xia, and A. Yakovlev, "MEMS-Based Runtime Idle Energy Minimization for Bursty Workloads in Heterogeneous Many-Core Systems," in *2018 IEEE 28th International Symposium on Power and Timing Modeling, Optimization and Simulation (PATMOS)*, 2018, pp. 198-205.
- [22] S. Cho, T. Chang, T. Yu, and C. H. Lee, "Smart electronic textiles for wearable sensing and display," *Biosensors*, vol. 12, no. 4, p. 222, 2022.
- [23] H. Alrudainy, R. Shafik, A. Mokhov, and A. Yakovlev, "Lifetime reliability characterization of N/MEMS used in power gating of digital integrated circuit," in *2017 IEEE International Symposium on Defect and Fault Tolerance in VLSI and Nanotechnology Systems (DFT)*, 2017, pp. 1-6.
- [24] T. Adam and T. S. Dhahi, "Nanosensors: Recent perspectives on attainments and future promise of downstream applications," *Process Biochemistry*, vol. 117, pp. 153-173, 2022.
- [25] M. E. Ali, M. M. Rahman, T. S. Dhahi, et al., "Nanostructured Materials: Bioengineering Platforms for Sensing Nucleic Acids," in *Encyclopedia of Smart Materials*, pp. 325-351, 2021.